Understanding random-walk dynamical phase coexistence through waiting times

David C. Stuhrmann [1] and Francesco Coghi [2,*]

[1]*Department of Physics, Stockholm University, Roslagstullsbacken 21, SE-106 91 Stockholm, Sweden*

[2]*Nordita, KTH Royal Institute of Technology and Stockholm University, Hannes Alfvéns väg 12, SE-106 91 Stockholm, Sweden*

(Received 13 August 2023; accepted 28 December 2023; published 22 January 2024)

We study the appearance of first-order dynamical phase transitions (DPTs) as "intermittent" coexisting phases in the fluctuations of random walks on graphs. We show that the diverging timescale leading to critical behavior is the waiting time to jump from one phase to another. This timescale is crucial for observing the system's relaxation to stationarity and demonstrate ergodicity of the system at criticality. We illustrate these results through three analytical examples which provide insights into random walks exploring random graphs.

DOI: 10.1103/PhysRevResearch.6.013077

I. INTRODUCTION

Random walks are arguably the most versatile model [1,2] to describe various transport processes in natural and artificial environments described as complex networks, including spreading of infections, propagation of information, search algorithms, and community detection [3–8]. Often, studies focus on dynamical observables whereby a single random walker hops on a graph and accumulates information related to some characteristics of the states visited over time. Among these dynamical observables we list first-passage times, currents, occupation times, and entropy production rates. Although the typical behavior of these dynamical observables obtained for long times is nowadays of easy interpretation, fluctuations and rare events, which are important over finite observation times, are less understood. In particular, among all possible rare events, dynamical phase transitions are strongly relevant.

Dynamical phase transitions (DPTs) are considered as changes in the random-walk fluctuation mechanisms. These have been observed in various models of single and many-particle interacting systems, involving the limit of certain parameters [9]. These are large system sizes [10–23], large particle numbers [24,25] and system volumes [26,27], or parameters associated to stochastic resetting [28–33], or again small rate/weak noise limits [34–37] and strong driving fields [38] of driven particle models. Recently, DPTs were observed in association with anomalous scaling of large deviations too [39–41].

DPTs are considered to arise whenever a nonanalytic (critical) behavior appears in large deviation functions, e.g., scaled cumulant generating functions (SCGFs) or rate functions. This critical behavior is surely a necessary condition, unlike time-reversal symmetry breakings [15–17,26], manifesting the divergence of a relevant timescale in the system. In the context of Markov processes, such a diverging timescale may arise as consequence of metastability [42–45] whereby the system slowly relaxes from a state that appears stationary at short times towards another that is genuinely stationary.

Nonetheless, it is important to note that a nondifferentiable point in a large deviation function is not enough to demonstrate a transition, such as phase coexistence, in the fluctuations of a dynamical observable [9,18,21]. When examining the time-dependent dynamics of a general diffusive system and considering a large deviation function of it, the latter might not exhibit all the characteristics of an equilibrium free energy—notably, large deviation functions of driven diffusive systems may be nonlocal in the density profile [46,47]—except in several cases as demonstrated in Refs. [16,17,34], where a Landau theory can be fully developed. Therefore, in such scenarios care must be taken and to link a kink in a SCGF to a physical transition one needs to better understand the phenomenology of the model being analysed, which may or may not show equilibrium-like phases [9,18,21].

In this paper, we show that when a nondifferentiable point appears in the SCGF of a time-additive observable of a random walk, the relevant diverging timescale—akin to a correlation length in equilibrium statistical mechanics—supporting the coexistence of two phases is the waiting time to jump from a phase to the other. Having two coexisting phases is intended at the level of single random-walk trajectories being "intermittent," i.e., the random walker keeps hopping from a phase to the other. In such a scenario, we will show that by opportunely rescaling the large deviation functions with the jump waiting time, the kink in the SCGF disappears, restoring a fully analytic function and the large deviation principle for the observable under examination. This means that the system once observed with the right timescale is still ergodic and therefore the walker visits all regions of the state space. We illustrate our findings through three

*francesco.coghi@su.se

analytical examples. Two of these are borrowed from a previous publication [22]—see also Appendix A for an overview of the main results of Ref. [22]—while one is entirely original. We believe these examples help to understand fluctuations of random walks exploring random graphs and the appearance of delocalization-localization DPTs [14,19,48]. It has been observed that in this context DPTs appear when the random walk (RW) observes a time additive cost that relates to local features of the random graph, such as the connectivity. As described toward the end of the paper, the three examples we discuss are progressively more suitable to catch the important features underlying these DPTs in RWs exploring Erdös-Rény random graphs, which are known to serve as a useful playground to study real-world networked systems [6,7,49].

II. MODEL SET UP, LARGE DEVIATIONS, AND THE DRIVEN PROCESS

We consider an n-time-step RW $X = (X_1, X_2, \ldots, X_\ell, \ldots, X_n)$ on a finite connected and undirected graph $G = (V, E)$ characterized by a set of states V of finite size N and a set of edges E. The RW dynamics is determined by the $N \times N$ stochastic transition matrix $\Pi = \{\pi_{ij}\}$ giving the probability π_{ij} of the RW to move from $X_\ell = i$ at time ℓ to $X_{\ell+1} = j$ at time $\ell + 1$. If i and j are not connected, then $\pi_{ij} = 0$; otherwise, $0 < \pi_{ij} \leqslant 1$.

At each time step ℓ the RW collects a certain "cost" (or "reward," "observable") related to the state of the system visited, namely $f(X_\ell)$. We focus on the dynamical observable that characterises the mean cost visited by a random-walk trajectory,

$$C_n = \frac{1}{n}\sum_{\ell=1}^{n} f(X_\ell), \tag{1}$$

with f a bounded function. Because the RW is ergodic—this is guaranteed by the properties of the graph G [50,51]—C_n converges to the ergodic average

$$\sum_{i\in V} \rho_i f(i) \coloneqq c^*, \tag{2}$$

where $\rho = \{\rho_i\}$ is the stationary distribution of the RW. For a finite observation time, the observable C_n is a random variable of the random-walk process and its distribution $P_{N,n}(C_n = c) \coloneqq P_{N,n}(c)$ is known to take the large deviation form [50–52]

$$P_{N,n}(c) = e^{-nI_N(c)+o(n)}, \tag{3}$$

with the time-leading behavior given by the nonnegative large deviation rate function $I_N(c)$ and $o(n)$ denoting corrections smaller than linear in n.

The large deviation rate function $I_N(c)$ can be hard to derive if the distribution $P_{N,n}(c)$ is unknown. In such a case, the rate function can be calculated by means of the so-called Gärtner–Ellis theorem [50–52]. This states that given a differentiable scaled cumulant generating function (SCGF)

$$\Psi_N(s) = \lim_{n\to\infty} \frac{1}{n} \ln \mathbb{E}[e^{nsC_n}], \tag{4}$$

the rate function I_N can be obtained via the following Legendre transform:

$$I_N(c) = s^* c - \Psi_N(s^*), \tag{5}$$

where s^* is the unique root of $\Psi'_N(s) = c$ [50]. In particular, given that the RW X is ergodic, the form of the SCGF simplifies to

$$\Psi_N(s) = \ln \zeta_s, \tag{6}$$

where ζ_s is the dominant eigenvalue of the so-called tilted matrix $\tilde{\Pi}_s = \{(\tilde{\pi}_s)_{ij}\}$, with components

$$(\tilde{\pi}_s)_{ij} = \pi_{ij} e^{sf(i)}. \tag{7}$$

The large deviation picture is complete once we understand how fluctuations $C_n = c$ are created in time. To do so, we construct the driven process [53–55] which, in this context, is a biased RW [19,54] whose transition probability matrix is given by

$$(\pi_s)_{ij} = \frac{(\tilde{\pi}_s)_{ij} r_s(j)}{r_s(i) e^{\Psi_N(s)}}, \tag{8}$$

where r_s is the right eigenvector associated with ζ_s. Under this process, the observable C_n is asymptotically distributed according to the canonical form

$$P^{(s)}_{N,n}(C_n = c) = \frac{e^{nsc} P_{N,n}(c)}{\mathbb{E}[e^{nsC_n}]}. \tag{9}$$

The driven process is well defined for finite N, still Markovian, and ergodic and can be interpreted as the effective dynamics of the subset of paths of the original RW leading to a fluctuation $C_n = c = \Psi'_N(s)$ [19,48].

III. DYNAMICAL PHASE TRANSITIONS: PHASE COEXISTENCE

Thanks to the Perron–Frobenious theorem, at finite N, the SCGF (4) and the rate function (5) are both analytic functions [50,51]. However, there is no general theorem that guarantees that for infinite N

$$\Psi(s) \coloneqq \lim_{N\to\infty} \Psi_N(s), \tag{10}$$

and its Legendre transform $I(c)$ are analytic. As mentioned in the introduction, there are many cases described in the literature where large deviation functions show singular points for such a limit.

Often, these singularities are interpreted as DPTs, viz. changes in the mechanisms that generate particular fluctuations of the observable C_n. In studying transitions, we follow a common practice used for equilibrium systems, as proposed by Ehrenfest [56]. Even for time-dependent models, we use the noncontinuous derivative of the SCGF to determine the order of the transition [57]. For this reason, a nondifferentiable point s_c in the SCGF $\Psi(s)$ is often referred to be a first-order DPT and therefore to signal an abrupt change in the fluctuations of C_n and, consequentially, the emergence of phase coexistence. However, it has recently been pointed out that such singular response of the SCGF is not strictly related with coexisting phases.

Indeed, other scenarios could arise, such as that of a slow system, or a pure ergodicity-breaking transition [18,21]. Applied to our context, in the former case, the random walker is simply extremely slow in moving from a phase to the other and the overall picture is that one of a RW slowly leaving a metastable state and being absorbed by a stable one. In the latter, we assist to the breaking of the large deviation principle for the observable under examination and therefore trajectories either visit one phase or the other (no mixing). Albeit their different physical interpretations, all these scenarios are commonly described by the blow-up of a characteristic timescale, namely $\tau(N)$, for $N \to \infty$.

Fully characterizing the timescale $\tau(N)$ allows one to properly rescale the Laplace parameter s around s_c, the SCGF $\Psi(s)$, and the rate function $I(c)$ as

$$\bar{s}(s) = \tau(N)(s - s_c), \tag{11}$$

$$\bar{\Psi}_N(\bar{s}) = \tau(N)[\Psi_N(s(\bar{s})) - \Psi(s_c)], \tag{12}$$

$$\bar{I}_N(c) = \tau(N) I(c), \tag{13}$$

such that $\bar{s}$ and $\bar{\Psi}_N(\bar{s})$ are now centered around 0 and we can rewrite (3) at leading order in n and for an observation time $n \gg \tau(N)$ [58] as $P_{N,n}(c) \approx e^{-\bar{n}\bar{I}_N(c)}$ with a new "speed" given by $\bar{n} := n/\tau(N)$. The system restores a large deviation principle and does not experience ergodicity breaking if the functions (12) and (13) are smooth for $N \to \infty$. We also anticipate here that the estimation of the relevant timescale $\tau(N)$ is obtained through an analytical expansion as the N-leading behavior of Eq. (12) (see the examples below for further details).

Incidentally, from Eq. (9) we can obtain the rate function and, by Legendre transform, the SCGF of the driven process which read

$$I_N^{(s^*)}(c) = I_N(c) - s^* c + \Psi_N(s^*), \tag{14}$$

$$\Psi_N^{(s^*)}(s) = \Psi_N(s + s^*) - \Psi_N(s^*), \tag{15}$$

having replaced s with s^* in Eq. (9) to indicate that we set the driven process at, in principle any, fixed s^*. Therefore, $\bar{\Psi}_N(\bar{s})$ in Eq. (12) and $\bar{I}_N(c)$ in Eq. (13) represent the $\tau(N)$-rescaled versions, for $s^* = s_c$, of Eqs. (15) and (14), respectively. In other words, the function $\bar{I}_N(c)$ is the limiting (for $N \to \infty$) rate function associated with the observable C_n of the driven process at s_c, opportunely rescaled by the diverging timescale $\tau(N)$. The latter provides an indication of the required simulation time for the driven process to relax and yield reliable statistics of C_n.

Finally, we argue that in the case of a two-phase coexistence, signalled by a nondifferentiable point in the SCGF $\Psi(s)$, the relevant timescale $\tau(N)$ is played by the waiting time to jump from a phase of the system to the other. In the following, we discuss three illustrative examples of RWs exploring graphs. For these, phase coexistence in the fluctuations of C_n is visualized by simulating the driven process, i.e., simply letting the random walk run over the state space, in the vicinity of the critical parameter s_c for large values of the parameter N and checking that RW trajectories are intermittent between the two phases (see, for instance, Fig. 3).

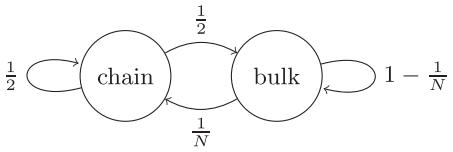

FIG. 1. Two-state random-walk model. Labels on edges refer to the transition probabilities between the states.

IV. EXAMPLES

A. Example 1: Two-state random walk

We start by considering a two-state RW. We name the two states "chain" and "bulk" and define the transition matrix to be

$$\Pi = \begin{pmatrix} \frac{1}{2} & \frac{1}{2} \\ \frac{1}{N} & 1 - \frac{1}{N} \end{pmatrix}, \tag{16}$$

such that, by increasing N, the RW spends on average more time in the "bulk" [59]. See Fig. 1 for a sketch of the states and the transition probabilities of the two-state RW model. Finally, the observable considered is (1) with $f(\text{chain}) = 1/N$ and $f(\text{bulk}) = 1$. In other words, the RW collects a normalized cost f—yielding an observable $C_n \in (0, 1]$—that is instrumental to the study of delocalization-localization DPTs of RWs on random graphs. In such a scenario the RW observes the mean-connectivity visited, which is approximately proportional to N, the number of nodes in the graph, when visiting the "bulk", and 1 when visiting a "chain" (we refer the reader to the last section of the paper for more details).

Typically, according to Eq. (2), the RW collects a cost $c^* = (2 + N^2)/(2N + N^2)$ which approaches 1 for large N. SCGF (4) and rate function (3) characterizing the long-time fluctuations of this observable have already been studied in Ref. [22]. In the limit $N \to \infty$ the SCGF $\Psi(s)$ develops a kink at $s = s_c := -\ln 2$ which leads to a linear section in $I(c)$ [see black curves in Figs. 2(a) and 2(b)]. For $s < s_c$, fluctuations arise from a longer time spent in "chain", while for $s > s_c$, fluctuations arise from a longer time spent in "bulk".

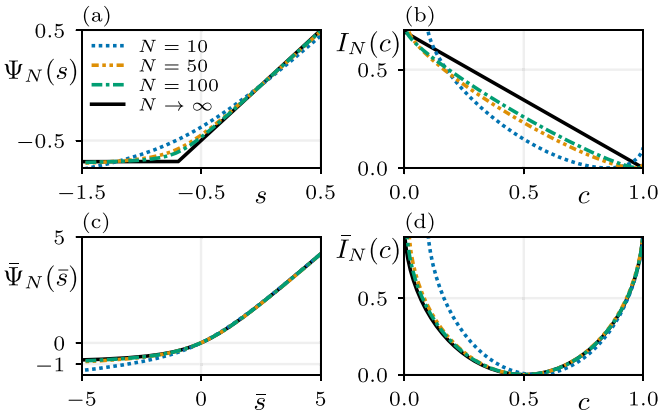

FIG. 2. Two-state RW: SCGFs $\Psi_N(s)$ in panel (a) and rate functions $I_N(c)$ in panel (b) at increasing values of N (colored curves) along with their limiting functions $\Psi(s)$ and $I(c)$ (black curves). Rescaled versions $\bar{\Psi}_N(\bar{s})$ and $\bar{I}_N(c)$ (colored curves), along with their limits $\bar{\Psi}(\bar{s})$ and $\bar{I}(c)$ (black curves) in panels (c) and (d).

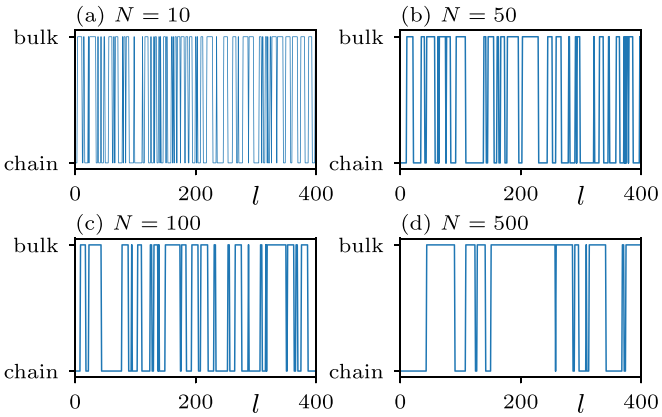

FIG. 3. From panels (a)–(d), intermittent trajectories visiting "bulk" and "chain" at increasing values of N for the two-state RW model. The larger the N the longer the waiting time to visit the other phase.

At the critical value s_c, the walker will spend half its time in "chain" and the other half in "bulk" as this typically realizes the fluctuation $C_n = 0.5$. In particular, in the long-time limit an intermittent behavior will arise whereby the walker, after spending a certain amount of time in "chain", will hop onto "bulk" and viceversa. For such a simple model, there is no other way the RW can create the fluctuation associated with s_c. We capture this intermittent behavior in Fig. 3 by simulating the driven process (8) with $s = s_c$ for finite but increasingly larger values of N.

Evidently, the larger the N the longer the time the RW waits before hopping to the other phase. This is the relevant—arguably the only for this model—timescale $\tau(N)$ that diverges for $N \to \infty$ and that leads to the appearance of a kink in the SCGF at s_c. The derivation of this effective timescale was accomplished in a previous work [22]—without much physical insights—by considering a general power-law form of $\tau(N)$, analytically expanding Eq. (12) in N and selecting the correct exponent for the power law such that the leading order of the expansion $\bar{\Psi}(\bar{s}) := \lim_{N\to\infty} \bar{\Psi}_N(\bar{s})$ is not trivial. For a detailed explanation of the derivation, we refer the reader to Ref. [22]. In Figs. 2(c) and 2(d) we display $\bar{\Psi}_N(\bar{s})$, its Legendre transform $\bar{I}_N(c)$, and their respective limits $\bar{\Psi}(\bar{s}) = \bar{s} + \sqrt{4+\bar{s}^2} - 2$ and $\bar{I}(c)$. Because of the smoothness of these last functions, in the timescale defined by $\tau(N)$ a large deviation principle is restored and fluctuations can be studied at s_c.

In Fig. 5(a) we plot $\tau(N) = \sqrt{N}$ and compare it with the mean waiting time to hop from "chain" to "bulk" and viceversa at increasing values of N. The average value of this quantity is obtained by simulating a driven process at $s = s_c$, counting the transitions unidirectionally between the states, and dividing the simulation time by the number of transitions. Noticeably, for this particular example only, the derivation of the driven process mean waiting time to hop from a phase to the other at criticality can also be carried out analytically using standard methods and show that it matches, at leading order, $\tau(N)$. To do so, one calculates the dominant eigenvalue and right eigenvector of the tilted matrix (7) and use that to build the finite-N driven process transition matrix (8), which, for

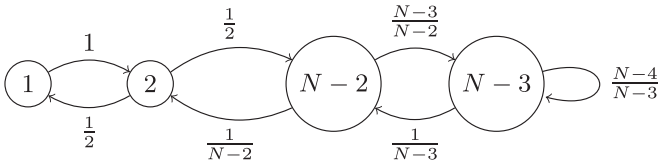

FIG. 4. The bulk-chain random-walk model reduced to four qualitatively different states. The edge labels are the transition probabilities where N is the number of nodes in the full graph. The nodes are labeled by their node degree and the different sizes of the nodes are used to distinguish between the chain (small) and the bulk (large).

convenience, is shown in Eq. (B1) in Appendix B. The mean waiting time to hop from "chain" to "bulk" ($\to$) and viceversa ($\leftarrow$) can easily be calculated following Refs. [60,61] and reads

$$\tau_{\to} = \frac{1}{(\pi_{-\ln(2)})_{1,2}} = \sqrt{N} + \frac{3-\ln 2}{2} + \frac{1-6\ln 2+(\ln 2)^2}{8\sqrt{N}} + O(N^{-2}), \tag{17}$$

$$\tau_{\leftarrow} = \frac{1}{(\pi_{-\ln(2)})_{2,1}} = \sqrt{N} + \frac{1+\ln 2}{2} + \frac{-7+4\ln 2+(\ln 2)^2}{8\sqrt{N}} + O(N^{-2}). \tag{18}$$

The leading orders in Eqs. (17) and (18) equal $\tau(N) = \sqrt{N}$ derived by analytical expansion of $\bar{\Psi}_N(\bar{s})$ as explained earlier. At the critical point $s = s_c$ and in the limit $N \to \infty$ the driven process is not ergodic and it will either visit one phase or the other, but will not be able to visit both because $\tau(N)$ diverges. For $s < s_c$ (case marked as s_-) it will only visit the "chain" phase and for $s > s_c$ (case s_+) it will only visit the "bulk" phase. To help the reader better understand the critical dynamics, we display in the following the leading order in N for $N \to \infty$ of the driven process transition matrices obtained from Eq. (B1):

$$\Pi_{s^-} = \begin{pmatrix} 1+O(N^{-1}) & O(N^{-1}) \\ 1-2e^s+O(N^{-1}) & 2e^s+O(N^{-1}) \end{pmatrix}, \tag{19}$$

$$\Pi_{s^+} = \begin{pmatrix} \frac{1}{2e^s}+O(N^{-1}) & 1-\frac{1}{2e^s}+O(N^{-1}) \\ O(N^{-1}) & 1+O(N^{-1}) \end{pmatrix}. \tag{20}$$

Furthermore, we remark that $\tau(N)$ has the same scaling form of the relaxation time of the driven process for $s = s_c$ calculated as the negative inverse of the spectral-gap logarithm of Eq. (8) [not displayed in Fig. 5(a) as fully overlapping $\tau(N)$]. Evidently, $\tau(N)$ well matches the analytical standard calculation leading to $\tau_{\to}$ and $\tau_{\leftarrow}$ and numerical simulations in Fig. 5(a) providing evidence that the critical timescale in a phase-coexistence scenario is determined by the waiting time between jumps.

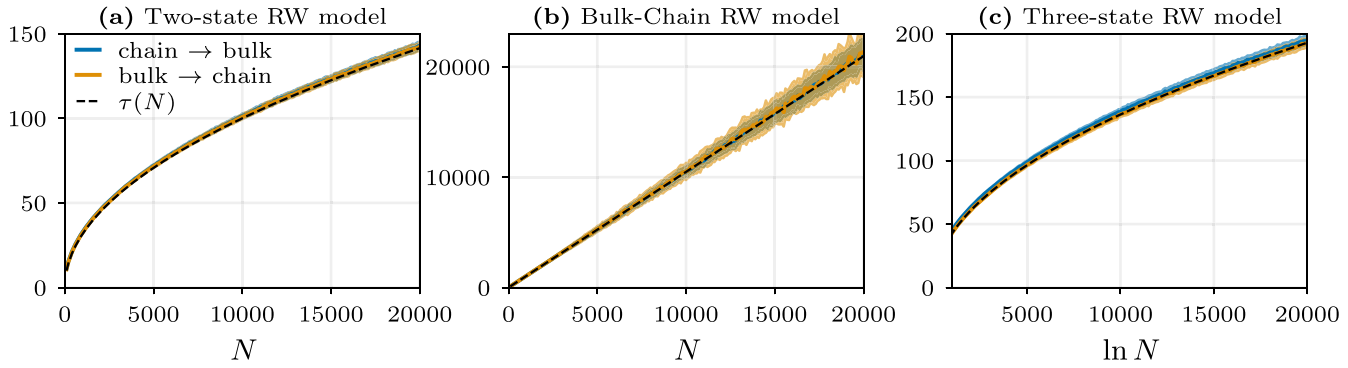

FIG. 5. Time rescalings $\tau(N)$ for the models investigated (black dashed lines) compared with mean waiting times to hop from one phase to the other for simulations of driven processes at $s = s_c$. The functional forms from panels (a)–(c) are $\sqrt{N}$, N and $(\ln N)^{1/2}$ where in panels (b) and (c), these are multiplied by the N-independent prefactors 1.048 and 1.364. For each N we run 100 simulations of $n = 10^6$ time steps (average marked as a solid colored line within one standard deviation).

B. Example 2: Bulk-chain random walk

We now focus on a slightly more complicated model. Different from the previous case, the fluctuation at the critical point can arise through two different mechanisms and we will show that the dominant one is an intermittent behavior supporting phase coexistence.

We analyze an unbiased RW with transition matrix

$$\pi_{ij} = \frac{a_{ij}}{k_i}, \tag{21}$$

with $A = \{a_{ij}\}$ representing the adjacency matrix of a graph of N nodes, i.e., $a_{ij} = 1$ if states i and j are connected and $a_{ij} = 0$ otherwise, and $k_i = \sum_{j=1}^{N} a_{ij}$ representing the connectivity of state i. The graph is composed by a fully connected bulk of $N-2$ nodes and a single chain of 2 nodes with connectivity 2 and 1 (we name this structure "dangling chain"). Because of symmetry, the graph has only 4 qualitatively different nodes. These are: the node of degree 1 at the edge of the chain, the node of degree 2 in the middle of the chain, the node of degree $N-2$ (gateway from now on) connecting bulk and chain, and a representative node of the bulk of degree $N-3$; see Fig. 4. On such a structure, the unbiased RW collects a cost of the form (1) with $f(X_\ell) = k_{X_\ell}/N$. As briefly discussed also in the previous example, the normalized cost chosen is useful to study the dynamical behavior of RWs on random graphs as explained in the last section of the paper.

As N increases, the RW spends more time in the bulk of the graph. The ergodic value, denoted by c^*, can be calculated and is given by $c^* = (-18 + 23N - 8N^2 + N^3)/[N(10 - 5N + N^2)]$. In large graphs, the RW tends to get lost in the bulk for a simple entropic reason: the higher the number of neighbors, the harder to find the dangling chain. Fluctuations of this model were already studied and we refer to Ref. [22] for details on the calculations. In Figs. 6(a) and 6(b) we report the SCGF $\Psi_N(s)$, the rate function $I_N(c)$, and their limiting behavior for $N \to \infty$. Evidently, a kink appears at $s_c := -(\ln 2)/2$. Similarly to the previous case, for $s < s_c$, the RW favors the dangling chain, while for $s > s_c$, it favors the bulk. At the critical value, it splits its time equally between both phases.

For this particular model there are two distinct ways the RW can split its time between bulk and dangling chain. On the one hand, the RW could keep hopping back and forth from the node of degree 2 and the gateway. On the other hand, it could spend some time in the dangling chain, then hop to the bulk and spend some time there before jumping back. Although both mechanisms are possible, the latter is more probable than the former. We checked this both estimating the probability of the two different events per unit time (as suggested in Ref. [21]) and by running simulations of the driven process at s_c for increasingly larger values of N.

We find that trajectories are intermittent in this case too. As they are qualitatively equivalent to the previous case we refer back to Fig. 3 for illustration purposes. The larger the N the longer the waiting time of the RW before it visits the other phase. By analytically expanding Eq. (12) in N as mentioned for the previous example we calculate $\tau(N) = N$ and the rescaled function $\bar{\Psi}(\bar{s})$ (its form is lengthy and not reported here, see Ref. [22]). We plot the latter, its Legendre transform, and numerical realizations for finite N given by Eqs. (12) and (13) in Figs. 6(c) and 6(d). Numerical realizations smoothly approach $\bar{\Psi}(\bar{s})$ endorsing the idea that at the relevant timescale $\tau(N)$ no critical behavior emerges.

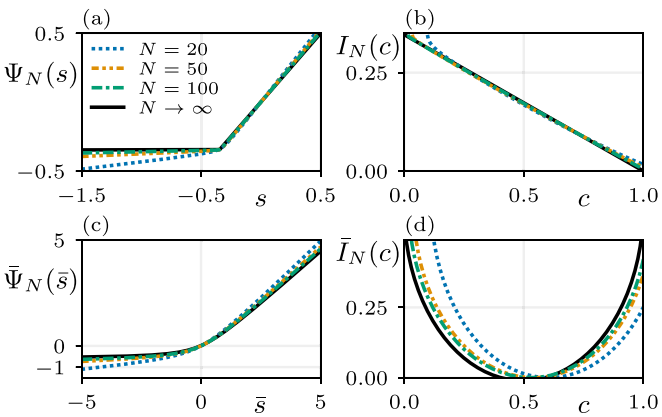

FIG. 6. Bulk-chain RW: SCGFs $\Psi_N(s)$ in panel (a) and rate functions $I_N(c)$ in panel (b) at increasing values of N (colored curves) along with their limiting functions $\Psi(s)$ and $I(c)$ (black curves). Rescaled versions $\bar{\Psi}_N(\bar{s})$ and $\bar{I}_N(c)$ (colored curves), along with their limits $\bar{\Psi}(\bar{s})$ and $\bar{I}(c)$ (black curves) in panels (c) and (d).

Eventually, in Fig. 5(b), we compare the form $\tau(N) = N$—corresponding to the relaxation timescale of the driven process in this case too—with numerical simulations of the driven process waiting time at the critical value s_c for different values of N. Since the analytically derived $\tau(N)$ captures only the leading functional form in N, we found that the N-independent prefactor 1.048 is needed to match the simulation data. We interpret the prefactor as a conversion factor from an absolute waiting time, the actual number of steps the random walk takes before hopping to the other phase, to a relative one, viz. measured in terms of the unit time given by the case $N = 1$. The numerical simulations strongly support the theory, providing further evidence that the waiting time is the key factor leading to a diverging timescale and dynamical phase coexistence. To better visualise the critical dynamics, in the following we display the leading order in N for $N \to \infty$ of the driven process transition matrices around the critical point s_c as calculated in Ref. [22]:

$$\Pi_{s^-} = \begin{pmatrix} 0 & 1 & 0 & 0 \\ 1 + O(N^{-1}) & 0 & O(N^{-1}) & 0 \\ 0 & -\frac{e^s}{3s} + O(N^{-1}) & 0 & 1 + \frac{e^s}{3s} \\ 0 & 0 & 1 - O(N^{-1}) & O(N^{-1}) \end{pmatrix}, \tag{22}$$

$$\Pi_{s^+} = \begin{pmatrix} 0 & 1 & 0 & 0 \\ \frac{e^{-2s}}{2} + O(N^{-1}) & 0 & \left(1 - \frac{e^{-2s}}{2}\right) + O(N^{-1}) & 0 \\ 0 & O(N^{-1}) & 0 & 1 + O(N^{-1}) \\ 0 & 0 & O(N^{-1}) & 1 + O(N^{-1}) \end{pmatrix}. \tag{23}$$

Similarly to Example 1, for $s < s_c$ (s_- case) the RW will only visit the "chain" of the state space, while for $s > s_c$ (s_+ case) the RW will only visit the "bulk".

C. Example 3: Three-state random walk

We consider a novel model of a RW over three states named "chain1", "chain2", and "bulk", characterized by the following transition matrix:

$$\Pi = \begin{pmatrix} 0 & 1 & 0 \\ \frac{1}{2} & 0 & \frac{1}{2} \\ 0 & \frac{\bar{k}}{\ln N} & 1 - \frac{\bar{k}}{\ln N} \end{pmatrix}, \tag{24}$$

with $\bar{k}$ and N being two positive parameters of the model such that $\bar{k} \leqslant \ln N$. Like the previous models, we can visualise the underlying graph as a dangling chain (composed by "chain1" and "chain2" states) linked to a bulk, which in this case is composed of a single self-looped state. Just like the bulk-chain RW model, increasing the value of N reduces the probability for the random walker to transition from the bulk to the dangling chain. However, due to the logarithmic dependence on N (which will be motivated in the following), this transition is relatively easier compared to the bulk-chain RW model. Finally, the RW collects also in this case an observable of the form (1) with $f(\text{chain1}) = 1$, $f(\text{chain2}) = 2$, and $f(\text{bulk}) = \bar{k}$; see Fig. 7. In this case too, the cost chosen is instrumental to the study of DPTs of RWs on random graphs (see next section for details).

The long-time behavior of the observable C_n is given by $c^* = [\bar{k}(5 + \ln N)]/(3\bar{k} + \ln N)$ and fluctuations can be studied with large deviation theory as outlined above. The SCGF $\Psi_N(s)$ in Eq. (4) can be calculated analytically but its form is lengthy and since it is not useful here is not displayed. Its limit for $N \to \infty$ in Eq. (10) can also be calculated and reads

$$\Psi(s) = \begin{cases} \frac{3s - \ln 2}{2} & \text{if} \quad s < s_c \\ \bar{k}s & \text{if} \quad s > s_c \end{cases}, \tag{25}$$

with a kink at

$$s_c = \frac{\ln 2}{3 - 2\bar{k}}. \tag{26}$$

These functions, along with their transforms, i.e., $I_N(c)$ and $I(c)$, are displayed in Figs. 8(a) and 8(b). Once again, when $s > s_c$, the RW will spend more time in the bulk ($c > c^*$), while for $s < s_c$ the RW favors the dangling chain ($c < c^*$).

At the critical value s_c the RW will spend half its time in the dangling chain and the other half in the bulk. Even in this case intermittent behavior arises as leading mechanism to generate fluctuations around the critical point s_c. We check this numerically by simulating the driven process (8) for increasingly larger values of N [62] and plot the trajectories in Fig. 9. Even in this scenario, as the value of N increases, the RW experience longer waiting times before transitioning to the other phase.

We derive $\bar{\Psi}(\bar{s})$ as leading-in-N behavior of Eq. (12) and the timescale $\tau(N)$. Analytically, we proceed by considering

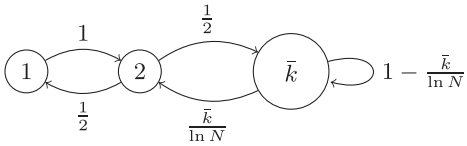

FIG. 7. The three-state random-walk model. The edge labels are the transition probabilities. The positive parameters $\bar{k}$ and N need to satisfy $\bar{k} \leqslant \ln N$. The nodes are labeled by their node degree and the different sizes of the nodes are used to distinguish between the chain (small) and the bulk (large).

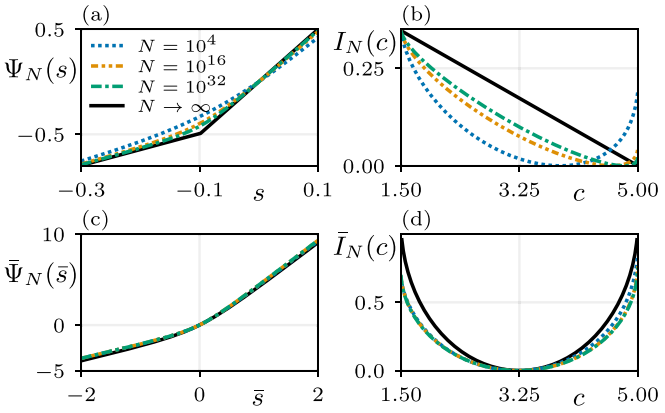

FIG. 8. Three-state RW: SCGFs $\Psi_N(s)$ in panel (a) and rate functions $I_N(c)$ in panel (b) at increasing values of N (colored curves) along with their limiting functions $\Psi(s)$ and $I(c)$ (black curves). Rescaled versions $\bar{\Psi}_N(\bar{s})$ and $\bar{I}_N(c)$ (colored curves), along with their limits $\bar{\Psi}(\bar{s})$ and $\bar{I}(c)$ (black curves) in panels (c) and (d).

the characteristic equation for the dominant eigenvalue $\lambda = e^{\Psi_N(s)}$ of the tilted matrix (7), i.e.,

$$(e^{\bar{k}s} - \lambda)(e^{3s} - 2\lambda^2) - \frac{e^{\bar{k}s}\ln\bar{k}}{\ln N}(e^{3s} + e^{2s}\lambda - 2\lambda^2) = 0. \tag{27}$$

We replace s and $\Psi_N(s)$ as functions of $\bar{s}$ and $\bar{\Psi}_N(\bar{s})$ inverting the relations given in Eqs. (11) and (12), respectively. Then, we make an educated guess and also replace $\tau(N) = (\ln N)^\alpha$ with $\alpha > 0$ and keep only the first order in $(\ln N)^{-\alpha}$ of Eq. (27). The value of $\alpha = 1/2$—the smallest possible—and the smooth function $\bar{\Psi}(\bar{s})$ are found imposing that the zero of the leading term of Eq. (27) is not the kinked function in Eq. (25). Figures 8(c) and 8(d) display the plots of $\bar{\Psi}(\bar{s})$ and $\bar{I}$, along with their finite-N approximations (12) and (13), respectively. The smoothness of the limiting functions suggests, once again, that there is a proper timescale in the large deviations such that no critical behavior is observed.

Eventually, we compare in Fig. 5(c) the scaling $\tau(N) = (\ln N)^{1/2}$ with the mean waiting time computed numerically

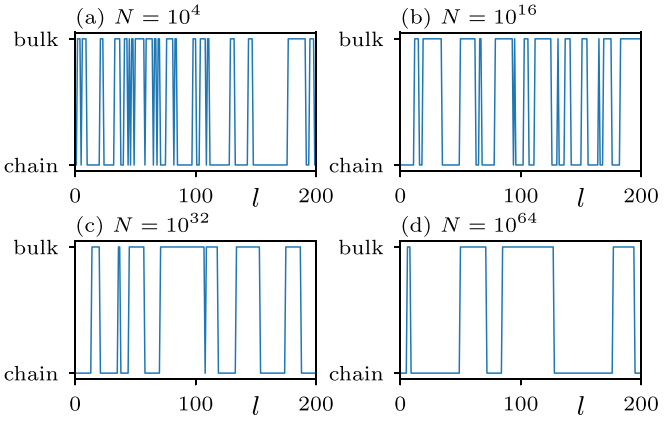

FIG. 9. From panels (a)–(d), intermittent trajectories visiting "bulk" and "chain" at increasing values of N for the three-state RW model. The larger the N the longer the waiting time to visit the other phase, although because of the logarithmic scale the change is less evident with respect to the two-state RW of Fig. 3.

by simulating driven processes with fixed $s = s_c$ for increasingly larger values of N. Once again, $\tau(N)$ corresponds to the relaxation timescale of the driven process and its form well matches numerical simulations of the waiting time multplied by an N-independent prefactor 1.364 similar to the bulk-chain RW example. We conclude that the waiting time is the leading diverging timescale supporting phase coexistence in the first-order DPT.

D. Implications for Erdös–Rényi random graphs

We have discussed three models that aim to capture the characteristics of a simplified version of an unbiased RW exploring an Erdös–Rényi (ER) random graph. Following Refs. [7,14,19], an ER graph is created by randomly connecting a fixed number N of nodes. The probability of connecting two nodes is determined by $\bar{k}/N$, where $\bar{k}$ represents the average connection of the graph. After generating the graph, only its largest connected component is retained and used as a base structure for a RW collecting a cost as in Eq. (1).

Large deviation theory has recently been employed to study this model [14,19]. In the case where $\bar{k}$ is sufficiently small, indications of a DPT have been identified between a phase characterized by bulk delocalization and another phase where the RW localises along dangling chains. Although no formal proof has been provided thus far for the existence of this DPT in the infinite-size ER graph ensemble, in recent times new interesting literature has appeared on phase coexistence in networked systems [37,48,63,64]. Understanding DPT behavior is crucial, not just for providing a more detailed description of the dynamics of stochastic dynamical systems, but also because real systems inherently experience fluctuations. This comprehension not only gives us insight into their dynamics but also provides a potential means, through the driven process, to control the occurrence of specific phases that could either benefit or harm the system.

The two-state and the bulk-chain RW models had previously been introduced [22] as analytical models aimed at explaining the delocalization-localization DPT in ER graphs (see Appendix A for a summary of the results relevant for our paper). Our three-state RW takes a further step in this direction. In the bulk-chain RW, increasing the size of N expands the bulk by adding fully connected nodes. However, this does not accurately reflect the behavior of adding a node in an ER graph, where the new node is not fully connected but, on average, maintains the same number of connections $\bar{k}$. Nevertheless, the presence of the new node increases the distance between a random node in the bulk and a node with degree 1 in a dangling chain. Since the average shortest distance between any two nodes of a random graph increases logarithmically with N, our third model considers the probability of transitioning from the bulk to the dangling chain to be inversely proportional to $\ln N$. Meanwhile, we maintain a constant cost (1) accumulated by the RW while visiting the bulk phase, which is equal to $\bar{k}$.

Indeed, this new model aligns more closely with the exploration of an ER random graph. Our three-state RW exhibits a delocalization-localization DPT that occurs at the critical value (26), which is inversely proportional to $\bar{k}$. This is expected in the ER graph too: The larger the $\bar{k}$ the more

connected the bulk, the smaller the tilting s to escape it. However, what is particularly striking about this transition is its speed, which goes like $(\ln N)^{1/2}$ and indicates the RW undergoes an exceptionally slow change in behavior as N increases.

V. CONCLUSION

We have investigated the appearance of first-order dynamical phase transitions in large deviation functions of simple discrete-time and space dynamical systems. The key finding of our study is that a kink in the scaled cumulant generating function of a time-additive observable for a random walk indicates phase coexistence when the dominant diverging timescale is the waiting time for the random walk to transition between phases. The characterization of such a timescale allows us to properly rescale large deviation functions and therefore rule out nonergodic behavior.

We have shown these results with three illustrative examples that work towards a better understanding of a potential delocalization-localization dynamical phase transition in random walks on Erdös–Rényi random graphs. Our results suggest that such a transition may appear at a remarkably slow rate, scaling as $O[(\ln N)^{1/2}]$, which poses significant challenges for numerical studies. Finally, we note that our work could serve as a theoretical ground to accelerate the learning process in numerical sampling schemes of large deviations near dynamical phase transitions [65–68].

ACKNOWLEDGMENTS

The authors are grateful to Supriya Krishnamurthy for support during the work. F.C. thanks Stephen Whitelam for insightful discussions at the Lawrence Berkeley National Lab and Giorgio Carugno and Hugo Touchette for valuable feedback on a first draft of the paper. This work has been partially supported by the Swedish Research Council Grant No. 638-2013-9243.

APPENDIX A: OVERVIEW OF THE RESULTS IN REF. [22]

We present a concise overview of the key findings from Ref. [22] without delving into the technical details of the calculations. We refer interested readers to the original paper for an in-depth analysis.

In Ref. [22], the authors explore the exact large deviation functions of a local dynamical observable [specifically, Eq. (1) in this study] for a random walk on two distinct models of connected and undirected graphs. These models, corresponding to the first two examples discussed earlier, capture essential physical aspects of the random-walk dynamics on Erdös–Rényi random graphs. Numerical investigations [14,19] already revealed a nondifferentiable point in the SCGF of the observable, indicating a sudden transition in the fluctuation mechanisms. This transition manifests as a shift from a fully delocalized state, where the random walk evenly explores the entire graph, to a fully localized state, where the random walk becomes confined to a specific portion of the graph. This observation supports the concept of a DPT as previosuly discussed.

In their study, the authors of Ref. [22] analytically derive the large deviation functions for the simplified models considered. In both cases, they demonstrate the occurrence of a DPT reminiscent of delocalization-localization behavior. What matters for our work is the form of the rescaled SCGFs presented in Ref. [22] and the determination of the relevant diverging timescale leading to a nondifferentiable point in the SCGFs. The authors employ a variational method in Ref. [22], formally discussed in Ref. [69], obtaining a polynomial equation that is then analytically expanded to reveal the crucial diverging timescale of the model (authors had no clue about the physical interpretation of such a timescale). Notably, this polynomial equation aligns with Example 3 mentioned earlier, representing the characteristic equation for the dominant eigenvalue of the pertinent tilted matrix. The timescales derived in Ref. [22] are discussed in Examples 1 and 2, namely, $\tau(N) = \sqrt{N}$ and $\tau(N) = N$, respectively. Example 3 introduces additional elements capturing other physical features in a simplified model, taking a step further in comprehending the emergence of a delocalization-localization DPT for random walks on random graphs.

APPENDIX B: FINITE-N FORM OF DRIVEN PROCESS TRANSITION MATRIX OF EXAMPLE 1

We display in the following the finite-N form of the driven process transition matrix of Example 1:

$$\Pi_s = \begin{pmatrix} \frac{2e^{\frac{s}{N}}}{\sqrt{e^{\frac{2s}{N}} - 4(1-\frac{3}{N})e^{s(1+\frac{1}{N})} + 4(1-\frac{1}{N})^2 e^{2s}} + e^{\frac{s}{N}} + 2(1-\frac{1}{N})e^{s}} & \frac{\sqrt{e^{\frac{2s}{N}} - 4(1-\frac{3}{N})e^{s(1+\frac{1}{N})} + 4(1-\frac{1}{N})^2 e^{2s}} - e^{\frac{s}{N}} + 2(1-\frac{3}{N})e^{s}}{4(1-\frac{2}{N})e^{s}} \\ \frac{1}{N}\frac{\sqrt{e^{\frac{2s}{N}} - 4(1-\frac{3}{N})e^{s(1+\frac{1}{N})} + 4(1-\frac{1}{N})^2 e^{2s}} + 3e^{\frac{s}{N}} - 2(1-\frac{1}{N})e^{s}}{\sqrt{e^{\frac{2s}{N}} - 4(1-\frac{3}{N})e^{s(1+\frac{1}{N})} + 4(1-\frac{1}{N})^2 e^{2s}} - (1-\frac{4}{N})e^{\frac{s}{N}} + 2(1-\frac{1}{N})e^{s}} & \frac{4(1-\frac{1}{N})e^{s}}{\sqrt{e^{\frac{2s}{N}} - 4(1-\frac{3}{N})e^{s(1+\frac{1}{N})} + 4(1-\frac{1}{N})^2 e^{2s}} + e^{\frac{s}{N}} + 2(1-\frac{1}{N})e^{s}} \end{pmatrix}. \tag{B1}$$

The form of the matrix is used in the main text to analytically derive the mean waiting time to jump from "chain" to "bulk" and viceversa as well as to run numerical simulations of the driven process at $s_c = -\ln 2$ for increasing values of N.

[1] G. Grimmet and D. Stirzaker, *Probability and Random Processes* (Oxford University Press, Oxford, UK, 2001).

[2] L. Gregory and L. Vlada, *Random Walk: A Modern Introduction* (Cambridge University Press, Cambridge, UK, 2010).

[3] B. D. Hughes, *Random Walks and Random Environments: Random Walks* (Oxford University Press, Oxford, UK, 1995).

[4] J. D. Noh and H. Rieger, Random walks on complex networks, Phys. Rev. Lett. **92**, 118701 (2004).

[5] R Burioni, B. Wang, Y.-X. Han, R. Burioni, and D. Cassi, Random walks on graphs: Ideas, techniques, and results, J. Phys. A: Math. Gen. **38**, R45 (2005).

[6] A. Barrat, M. Barthélemy, and A. Vespignani, *Dynamical Processes on Complex Networks* (Cambridge University Press, Cambridge, UK, 2008).

[7] M. E. J. Newman, *Networks: An Introduction* (Oxford University Press, Oxford, UK, 2010).

[8] N. Masuda, M. A. Porter, and R. Lambiotte, Random walks and diffusion on networks, Phys. Rep. **716-717**, 1 (2017).

[9] S. Whitelam, Comment on the literature definition(s) of "dynamical phase transition," arXiv:2112.09107v1.

[10] T. Bodineau and B. Derrida, Distribution of current in nonequilibrium diffusive systems and phase transitions, Phys. Rev. E **72**, 066110 (2005).

[11] L. Bertini, A. De Sole, D. Gabrielli, G. Jona-Lasinio, and C. Landim, Current fluctuations in stochastic lattice gases, Phys. Rev. Lett. **94**, 030601 (2005).

[12] J. P. Garrahan, R. L. Jack, V. Lecomte, E. Pitard, K. Van Duijvendijk, and F. van Wijland, Dynamical first-order phase transition in kinetically constrained models of glasses, Phys. Rev. Lett. **98**, 195702 (2007).

[13] S. Vaikuntanathan, T. R. Gingrich, and P. L. Geissler, Dynamic phase transitions in simple driven kinetic networks, Phys. Rev. E **89**, 062108 (2014).

[14] C. De Bacco, A. Guggiola, R. Kühn, and P. Paga, Rare events statistics of random walks on networks: Localisation and other dynamical phase transitions, J. Phys. A: Math. Theor. **49**, 184003 (2016).

[15] O. Shpielberg and E. Akkermans, Le chatelier principle for out-of-equilibrium and boundary-driven systems: Application to dynamical phase transitions, Phys. Rev. Lett. **116**, 240603 (2016).

[16] Y. Baek, Y. Kafri, and V. Lecomte, Dynamical symmetry breaking and phase transitions in driven diffusive systems, Phys. Rev. Lett. **118**, 030604 (2017).

[17] Y. Baek, Y. Kafri, and V. Lecomte, Dynamical phase transitions in the current distribution of driven diffusive channels, J. Phys. A: Math. Theor. **51**, 105001 (2018).

[18] S. Whitelam, Large deviations in the presence of cooperativity and slow dynamics, Phys. Rev. E **97**, 062109 (2018).

[19] F. Coghi, J. Morand, and H. Touchette, Large deviations of random walks on random graphs, Phys. Rev. E **99**, 022137 (2019).

[20] B. Buča, J. P. Garrahan, T. Prosen, and M. Vanicat, Exact large deviation statistics and trajectory phase transition of a deterministic boundary driven cellular automaton, Phys. Rev. E **100**, 020103(R) (2019).

[21] S. Whitelam and D. Jacobson, Varied phenomenology of models displaying dynamical large-deviation singularities, Phys. Rev. E **103**, 032152 (2021).

[22] G. Carugno, P. Vivo, and F. Coghi, Delocalization-localization dynamical phase transition of random walks on graphs, Phys. Rev. E **107**, 024126 (2023).

[23] R. Gutiérrez and C. Pérez-Espigares, Dynamical phase transition to localized states in the two-dimensional random walk conditioned on partial currents, Phys. Rev. E **104**, 044134 (2021).

[24] T. Nemoto, É. Fodor, M. E. Cates, R. L. Jack, and J. Tailleur, Optimizing active work: Dynamical phase transitions, collective motion, and jamming, Phys. Rev. E **99**, 022605 (2019).

[25] T. Agranov, M. E. Cates, and R. L. Jack, Tricritical behavior in dynamical phase transitions, Phys. Rev. Lett. **131**, 017102 (2023).

[26] G. Bunin, Y. Kafri, and D. Podolsky, Non-differentiable large-deviation functionals in boundary-driven diffusive systems, J. Stat. Mech.: Theory Exp. (2012) L10001.

[27] K. Proesmans, R. Toral, and C. Van den Broeck, Phase transitions in persistent and run-and-tumble walks, Physica A **552**, 121934 (2020).

[28] R. J. Harris and H. Touchette, Phase transitions in large deviations of reset processes, J. Phys. A: Math. Theor. **50**, 10LT01 (2017).

[29] M. Zamparo, Large deviations in renewal models of statistical mechanics, J. Phys. A: Math. Theor. **52**, 495004 (2019).

[30] F. Coghi and R. J. Harris, A large deviation perspective on ratio observables in reset processes: Robustness of rate functions, J. Stat. Phys. **179**, 131 (2020).

[31] M. Zamparo, Statistical fluctuations under resetting: Rigorous results, J. Phys. A: Math. Theor. **55**, 484001 (2022).

[32] F. Mori, K. S. Olsen, and S. Krishnamurthy, Entropy production of resetting processes, Phys. Rev. Res. **5**, 023103 (2022).

[33] M. Zamparo and M. Semeraro, Large deviations for quadratic functionals of stable Gauss-Markov chains and entropy production, J. Math. Phys. **64**, 023302 (2023).

[34] Y. Baek and Y. Kafri, Singularities in large deviation functions, J. Stat. Mech.: Theory Exp. (2015) P08026.

[35] P. Tsobgni Nyawo and H. Touchette, Large deviations of the current for driven periodic diffusions, Phys. Rev. E **94**, 032101 (2016).

[36] K. Proesmans and B. Derrida, Large-deviation theory for a Brownian particle on a ring: A WKB approach, J. Stat. Mech.: Theory Exp. (2019) 023201.

[37] L. Di Gaetano, G. Carugno, F. Battiston, and F. Coghi, Dynamical fluctuations in a minimal model of higher-order networks, arXiv:2303.18169v1.

[38] C. P. Espigares, P. L. Garrido, and P. I. Hurtado, Dynamical phase transition for current statistics in a simple driven diffusive system, Phys. Rev. E **87**, 032115 (2013).

[39] D. Nickelsen and H. Touchette, Anomalous scaling of dynamical large deviations, Phys. Rev. Lett. **121**, 090602 (2018).

[40] N. R. Smith, Anomalous scaling and first-order dynamical phase transition in large deviations of the Ornstein-Uhlenbeck process, Phys. Rev. E **105**, 014120 (2022).

[41] A. L. Stella, A. Chechkin, and G. Teza, Anomalous dynamical scaling determines universal critical singularities, Phys. Rev. Lett. **130**, 207104 (2023).

[42] H. Larralde and F. Leyvraz, Metastability for Markov processes with detailed balance, Phys. Rev. Lett. **94**, 160201 (2005).

[43] H. Larralde, F. Leyvraz, and D. P. Sanders, Metastability in Markov processes, J. Stat. Mech.: Theory Exp. (2006) P08013.

[44] K. Macieszczak, M. Guta, I. Lesanovsky, and J. P. Garrahan, Towards a theory of metastability in open quantum dynamics, Phys. Rev. Lett. **116**, 240404 (2016).

[45] K. Macieszczak, D. C. Rose, I. Lesanovsky, and J. P. Garrahan, Theory of classical metastability in open quantum systems, Phys. Rev. Res. **3**, 033047 (2021).

[46] B. Derrida, J. L. Lebowitz, and E. R. Speer, Free energy functional for nonequilibrium systems: An exactly solvable case, Phys. Rev. Lett. **87**, 150601 (2001).

[47] J. Tailleur, J. Kurchan, and V. Lecomte, Mapping nonequilibrium onto equilibrium: The macroscopic fluctuations of simple transport models, Phys. Rev. Lett. **99**, 150602 (2007).

[48] R. Gutiérrez and C. Pérez-Espigares, Generalized optimal paths and weight distributions revealed through the large deviations of random walks on networks, Phys. Rev. E **103**, 022319 (2021).

[49] V. Latora, V. Nicosia, and G. Russo, *Contemporary Physics* (Cambridge University Press, Cambridge, UK, 2017).

[50] H. Touchette, The large deviation approach to statistical mechanics, Phys. Rep. **478**, 1 (2009).

[51] A. Dembo and O. Zeitouni, *Large Deviations Techniques and Applications*, Stochastic Modelling and Applied Probability, Vol. 38 (Springer, Berlin, 2010).

[52] F. den Hollander, *Large Deviations* (American Mathematical Society, Providence, RI, 2000).

[53] R. Chetrite and H. Touchette, Nonequilibrium microcanonical and canonical ensembles and their equivalence, Phys. Rev. Lett. **111**, 120601 (2013).

[54] R. Chetrite and H. Touchette, Nonequilibrium Markov processes conditioned on large deviations, Ann. Henri Poincaré **16**, 2005 (2015).

[55] R. Chetrite and H. Touchette, Variational and optimal control representations of conditioned and driven processes, J. Stat. Mech.: Theory Exp. (2015) P12001.

[56] P. Ehrenfest, *Phasenumwandlungen im ueblichen und erweiterten Sinn, classifiziert nach den entsprechenden Singularitaeten des thermodynamischen Potentiales* (NV Noord-Hollandsche Uitgevers Maatschappij, 1933).

[57] Sometimes scientists define the order of the DPT by looking at the rate function rather than the SCGF. The SCGF $\Psi(s)$ is, arguably, closer in form to a Helmoltz (canonical) free energy although this, strictly speaking, would be obtained by dividing $-\Psi(-s)$ by the Laplace parameter s [50]. We do not do that because $\Psi(s)$ is already, conveniently, convex. Furthermore, because of the Legedre transform (5) connecting the SCGF to the rate function, a DPT of order n in the SCGF will be interpreted as of order $n+1$ in the rate function.

[58] This, in turn, explains the order of the limits taken, which often do not commute.

[59] Notice that the parameter N here is not the size of the graph (as considered when setting up the model). However, it will play the same role.

[60] G. Rubino and B. Sericola, Sojourn times in finite Markov processes, J. Appl. Probab. **26**, 744 (1989).

[61] K. Sekimoto, Derivation of the First Passage Time Distribution for Markovian Process on Discrete Network, arXiv:2110.02216.

[62] Regrettably, in the case of this specific example, obtaining the leading order in N for the transition matrix of the driven process is technically challenging and even after many attempts using Mathematica we cannot derive it.

[63] I. Neri and F. L. Metz, Linear stability analysis of large dynamical systems on random directed graphs, Phys. Rev. Res. **2**, 033313 (2020).

[64] C. W. Lynn, L. Papadopoulos, A. E. Kahn, and D. S. Bassett, Human information processing in complex networks, Nat. Phys. **16**, 965 (2020).

[65] T. Nemoto, R. L. Jack, and V. Lecomte, Finite-size scaling of a first-order dynamical phase transition: Adaptive population dynamics and an effective model, Phys. Rev. Lett. **118**, 115702 (2017).

[66] G. Ferré and H. Touchette, Adaptive sampling of large deviations, J. Stat. Phys. **172**, 1525 (2018).

[67] F. Coghi and H. Touchette, Adaptive power method for estimating large deviations in Markov chains, Phys. Rev. E **107**, 034137 (2023).

[68] J. Yan, H. Touchette, and G. M. Rotskoff, Learning nonequilibrium control forces to characterize dynamical phase transitions, Phys. Rev. E **105**, 024115 (2022).

[69] G. Carugno, P. Vivo, and F. Coghi, Graph-combinatorial approach for large deviations of Markov chains, J. Phys. A: Math. Theor. **55**, 295001 (2022).